

## Elimination of Te precipitates from CdTe wafers

This content has been downloaded from IOPscience. Please scroll down to see the full text.

1995 Semicond. Sci. Technol. 10 870

(<http://iopscience.iop.org/0268-1242/10/6/020>)

View [the table of contents for this issue](#), or go to the [journal homepage](#) for more

Download details:

IP Address: 148.228.150.246

This content was downloaded on 07/01/2014 at 22:52

Please note that [terms and conditions apply](#).

# Elimination of Te precipitates from CdTe wafers

N V Sochinskii†‡, E Diéguez†, U Pal§, J Piqueras§,  
P Fernández§ and F Agulló-Rueda||

† Departamento de Física de Materiales, Universidad Autónoma, 28049 Madrid, Spain

§ Departamento de Física de Materiales, Facultad de Física, Universidad Complutense, 28040 Madrid, Spain

|| Instituto de Ciencia de Materiales de Madrid (CSIC), Campus de Cantoblanco, 28049 Madrid, Spain

Received 28 December 1994, accepted for publication 14 February 1995

**Abstract.** Undoped and doped CdTe wafers have been thermally annealed in Ga melt, or in Cd vapour or in a vacuum to eliminate Te precipitates from the volume of the wafers. The effect of annealing conditions on the transformation of Te precipitates has been studied by Raman scattering (RS) and cathodoluminescence (CL) techniques. The RS and CL spectra of the as-grown and annealed wafers are discussed in connection with the doping and native structural defects and residual impurities.

The kinetics of elimination of Te precipitates was found to be similar in the undoped and doped wafers. The rate of elimination is the highest for the annealing in Ga melt. Precipitate-free wafers have been obtained by annealing in Ga melt at 600 °C for 24 h. Simultaneously with the elimination of Te precipitates, Ga melt causes the in-diffusion of Ga atoms into the wafers. This implies that annealing in Ga melt could be a superior procedure for the elimination of Te precipitates from CdTe wafers in which Ga doping is not important or is desired.

## 1. Introduction

The use of CdTe wafers, as well as the ternary compounds based on CdTe, for numerous sensor applications is restricted by Te precipitates which are distributed randomly over the whole volume of the wafers [1–4]. The presence of Te precipitates in CdTe crystals grown from a binary Cd–Te melt is due to the known peculiarities of the phase diagram of CdTe, which are a Te-rich composition in the vicinity of the CdTe melting point and a strong retrograde character of solidus on the Te-rich side of homogeneity region [5]. The Te precipitates create some technological problems for the post-growth stoichiometry control of CdTe. The main one is an unpredictable transformation of Te precipitates during the different thermal treatments of CdTe wafers. These treatments are widely required to get a dopant indiffusion [6–8], to fabricate the ohmic contacts [9, 10] and to suppress an out-diffusion of residual impurities from CdTe substrates during  $\text{Hg}_{1-x}\text{Cd}_x\text{Te}$  epitaxial growth [11].

The annealing of the as-grown CdTe wafers in Cd vapour [12, 13] or in a graded temperature field [4] has been proposed to reduce the concentration

of Te precipitates. The reduced concentration of Te precipitates in Cl-doped CdTe crystals has also been reported [3]. Nevertheless, the complete elimination of Te precipitates from the whole volume of CdTe wafers still remains a problem.

In the past, several characterization techniques like infrared microscopy [1–3], Raman scattering (RS) [12], infrared spectroscopy [12, 13] and calorimetry [3] have been employed to study the Te precipitates in CdTe wafers. Recently, we have shown that the combined use of the RS and cathodoluminescence (CL) techniques yields more information on the transformation of Te precipitates in the volume of CdTe wafers, and the possibility of eliminating Te precipitates by thermal annealing procedures has also been reported [14]. In this paper we present the extended results of RS and CL studies on the elimination of Te precipitates by annealing of CdTe wafers in Ga melt and we discuss the effect of the annealing procedure on the spatial distribution of structural defects in the undoped and doped CdTe wafers.

## 2. Experiment

### 2.1. Annealing procedure

The bulk CdTe crystals, undoped and doped with Mn or Sb or Cl, were grown by the vertical Bridgman method.

‡ On leave from: Institute of Semiconductor Physics, pr. Nauki 45, Kiev 252028, Ukraine and New Semiconductors, Inc., Kiev 254210, PO Box 222, Ukraine.

The growth parameters and the crystal characteristics have been reported elsewhere [7]. The single-crystalline wafers were cut with the (111) orientation and with a size of about  $20 \times 20 \times 1.5 \text{ mm}^3$ . In a conventional way [7, 10], the wafers were chemically polished and washed to remove the surface damage. A layer of pure Ga (6 N) of thickness about 1 mm was deposited at room temperature (RT) on one side of a wafer by spreading Ga drops. The annealing procedures were carried out in the evacuated quartz ampoules at temperature of  $600^\circ\text{C}$  for a time period of 2 or 24 h.

In order to confirm the effect of Ga melt, few CdTe wafers were annealed at the same time-temperature conditions in Cd vapour and in an evacuated ampoule without Ga. After annealing, an ampoule was removed from the hot furnace and cooled in air.

## 2.2. RS and CL measurements

Before the measurements, the as-grown and annealed CdTe wafers were cleaved perpendicularly to the wafer surface. The RS and CL spectra and the CL images were studied on the cleaved surfaces in order to get information on the whole volume of the wafers. By recording RS spectra from the cleaved surfaces we have also avoided the possible influence of the chemical treatment of the wafers, which can disable the use of RS for the study of Te precipitates because of the presence of a residual surface layer of polycrystalline Te after the treatment [15].

RS spectra were obtained with an Ar ion laser ( $\lambda = 514.4 \text{ nm}$ ) and recorded with a Dilor XY spectrometer at RT. The dimensions of the laser beam spot on the sample surface were of few micrometres (microregime) or about  $5 \text{ mm} \times 100 \mu\text{m}$  (macroregime). In the microregime the focusing of the laser beam and the collection of scattered light were done through a microscope. The laser power was kept below 2 mW and 100 mW for the micro- and macroregimes respectively to avoid surface damage.

CL spectra and images were studied in a Hitachi S-2500 scanning electron microscope (SEM) at temperatures in the range from 80 K to RT. A North Coast EO-817 germanium detector was used for the spectral and panchromatic CL measurements as has been previously reported [16]. In analogy with [17], CL spectra were recorded with a focused and defocused electron beam to detect the radiative defect centres with different concentrations.

## 3. Results and discussion

### 3.1. RS data

Figure 1 shows the RS spectra of the as-grown CdTe wafers on which the annealing experiments have been done. Over the whole volume of the wafers the RS spectra consist of two peaks at  $125 \text{ cm}^{-1}$  and  $143 \text{ cm}^{-1}$ , which have been attributed to the Te precipitates in a crystalline form [12, 15]. The CdTe-related peaks

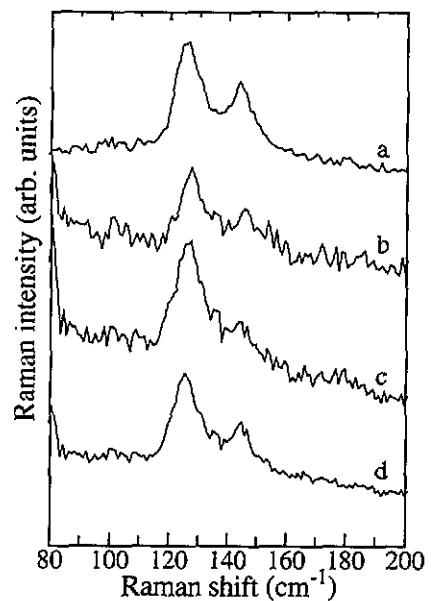


**Figure 1.** RS spectra recorded in the microregime from a cross section of as-grown CdTe wafers: (a) undoped, (b) doped with Mn ( $N_{\text{Mn}} = 10^{18} \text{ cm}^{-3}$ ), (c) doped with Sb ( $N_{\text{Sb}} = 10^{18} \text{ cm}^{-3}$ ), (d) doped with Cl ( $N_{\text{Cl}} = 10^{20} \text{ cm}^{-3}$ ).

corresponding to the transversal optical (TO) phonon at  $142 \text{ cm}^{-1}$  and the longitudinal optical (LO) phonon at  $170 \text{ cm}^{-1}$  were not seen in the microregime. The heavy doping with the different impurities did not significantly affect the position and intensity of the Te-related peaks.

After the 2 h annealing in the Ga melt a similar transformation of the RS spectra was found to take place in the volume of the undoped and doped CdTe wafers (figure 2). In the central part of the cross section of the wafers, the intensity of the  $125 \text{ cm}^{-1}$  peak decreased by a factor of two to three and became equal to or less than the intensity of the  $143 \text{ cm}^{-1}$  peak (figure 2, curve a). Simultaneously, the intensities of both Te-related peaks increased by a factor of two to five near the wafers surface which was in contact with the Ga melt (figure 2, curve b). Near the opposite surface of the wafers, which was exposed to vacuum, the initial RS spectra did not change remarkably after the 2 h annealing.

The 24 h annealing in the Ga melt caused other dramatic modification of the RS spectra, which were found to be similar in the undoped and doped CdTe wafers as after the 2 h annealing. In the microregime (figure 3), the Te-related peaks disappeared over the whole volume of the wafers. Only within a  $100\text{--}200 \mu\text{m}$  thick region at the surface which was not in contact with the Ga melt, i.e. it was exposed to a vacuum, were the RS spectra similar to the one shown in figure 2(b), demonstrating an increase of intensity of the Te-related peaks.

In the macroregime (figure 4), the modification of the RS spectra was more apparent after the 24 h Ga melt annealing. The Te-related peaks are not present as in the case of the microregime (figure 3), and the RS spectra are dominated by the TO and LO phonon peaks of CdTe over the whole volume of the wafers with the exception of the near-surface regions.

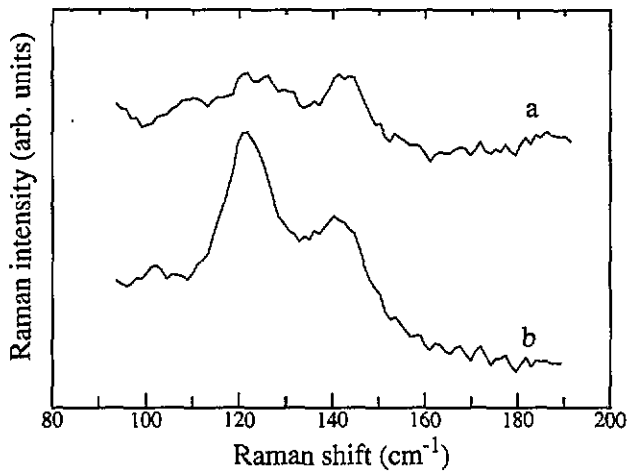


**Figure 2.** RS spectra recorded in the microregime from a cross section of the CdTe wafer annealed in the Ga melt at 600°C for 2 h: (a) in the central part of the cross section; (b) in the region about 100  $\mu\text{m}$  away from the water surface which was in contact with the Ga melt.

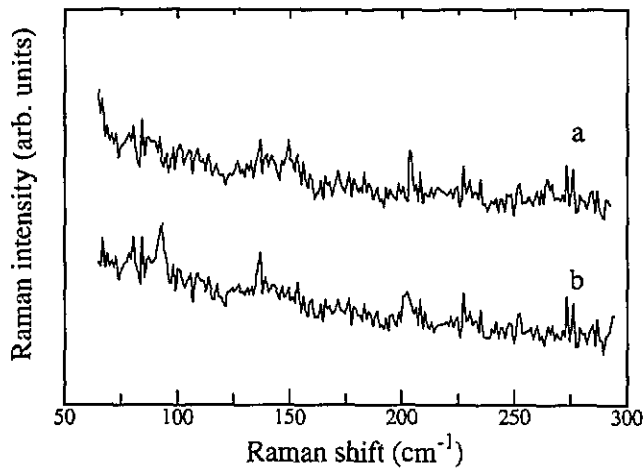


**Figure 3.** RS spectra recorded in the microregime from a cross section of the CdTe wafer annealed in Ga melt at 600°C for 24 h: (a) in the central part of the cross section; (b) in the region about 200  $\mu\text{m}$  away from the water surface which was in contact with the Ga melt.

Finally, it is worth mentioning that the 125  $\text{cm}^{-1}$  peak seems to be a favourable indicator for monitoring Te precipitates in the volume of CdTe wafers by the RS technique.

### 3.2. CL data

Like the RS spectra, the CL images and spectra have not revealed any significant effect of doping on the transformation of Te precipitates. Figure 5 shows the typical CL images of the as-grown (a) and annealed (b)–(d) CdTe wafers, corresponding to the regions of the wafer cross sections from which the RS and CL spectra were recorded. While the as-grown wafers were of a good structural quality estimated by x-ray measurements [7], their CL images exhibited a random spatial distribution of Te precipitates over the whole volume (figure 5(a)).

After the 2 h annealing in the Ga melt, a significant improvement of the CL image contrast was usually

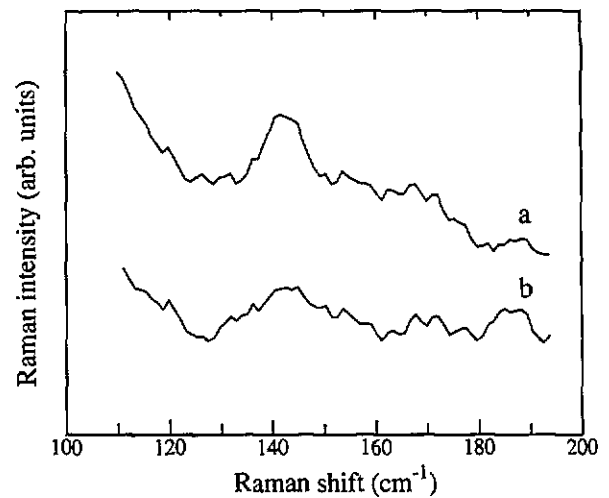


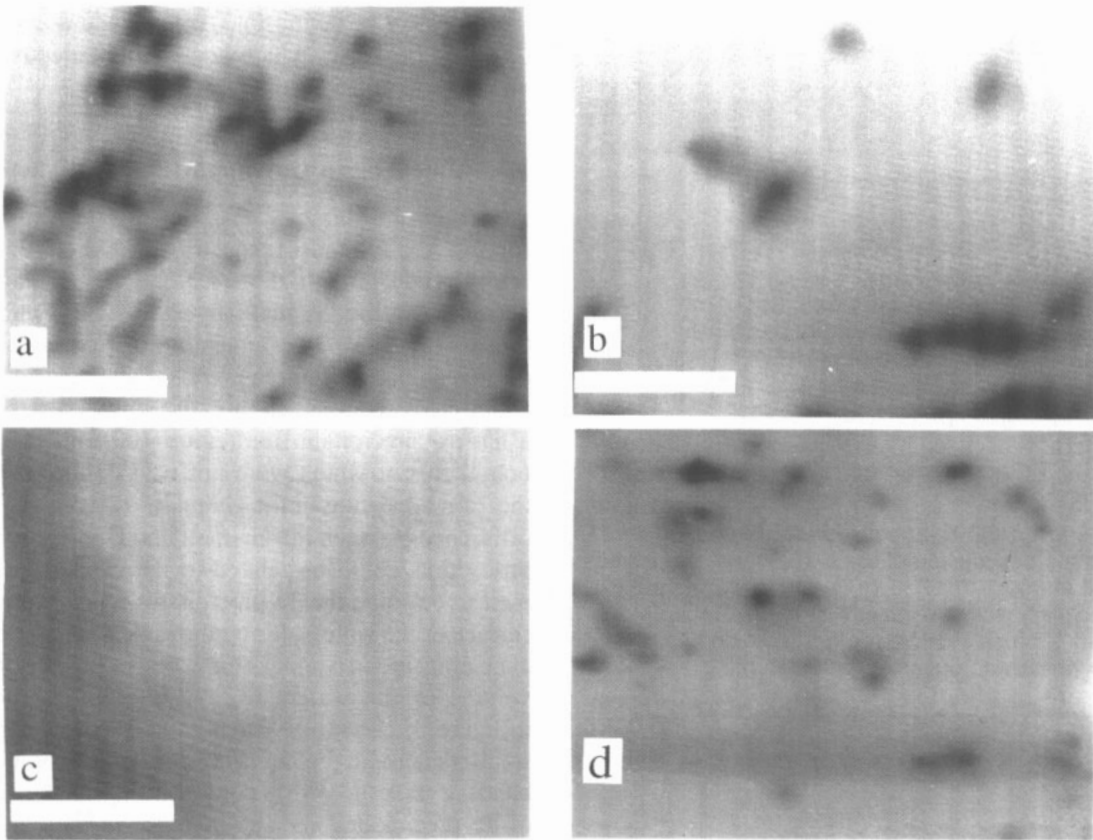
**Figure 4.** RS spectra recorded in the macroregime from a cross section of the CdTe wafer annealed in Ga melt at 600°C for 24 h: (a) in the central part of the cross section; (b) in the region about 200  $\mu\text{m}$  away from the water surface which was in contact with the Ga melt.

observed in the central part of the wafer cross sections, demonstrating the disappearance of small ( $< 10 \mu\text{m}$ ) Te precipitates and a reduction in the density of structural defects in the space between precipitates (figure 5(b)). On the contrary, a strong increase in the concentration of Te precipitates was seen near the surface of the wafers which was in contact with the Ga melt. This precipitate-rich region extends up to 200  $\mu\text{m}$  away from the surface. Simultaneously, the initial CL image did not change significantly near the opposite surface of the wafers, which were exposed in a vacuum.

After the 24 h annealing in the Ga melt, a complete disappearance of Te precipitates was found to take place over the whole volume of the wafers, with the exception of the regions near the surfaces. That provided a clear precipitate-free CL image throughout the main part of the wafer thickness, without any remarkable features. Within a distance of about 100  $\mu\text{m}$  from the wafer surface in contact with the Ga melt, the CL image showed a high density of Te precipitates. Interestingly, it was observed near this surface that the boundary between the precipitate-free and precipitate-rich regions was usually well defined (figure 5(c)). Some increase in the concentration of Te precipitates was also seen near the opposite surface of the wafers, which were exposed in a vacuum (figure 5(d)). That can be attributed to the surface gettering effect.

Figure 6 shows the typical CL spectra recorded from a cleaved surface of as-grown undoped CdTe wafers. The CL spectra consist of three emission bands with the maxima peaked at about 1.13, 1.4 and 1.54 eV. These bands have been attributed to the different complex defects in CdTe such as Te vacancy–impurity complexes (1.13 eV band), Cd vacancy–impurity pairs (1.4 eV band) and donor–acceptor pairs (1.54 eV band) [7, 8, 17 and references therein]. The intensity of CL bands was about the same over all the volume of as-grown wafers.

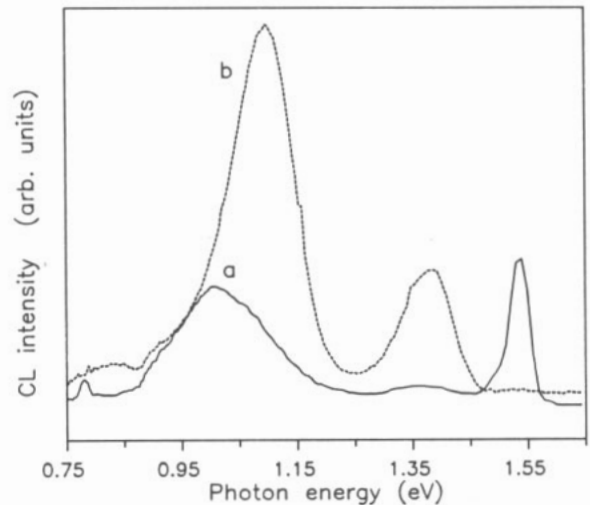
After annealing in the Ga melt, the CL spectra were found to be modified and different in the different regions



**Figure 5.** Panchromatic CL images of a cross section of CdTe wafers at 80 K: (a) as-grown; (b) in the central part of cross section after the annealing in the Ga melt at 600 °C for 2 h; (c) near the water surface which was in contact with the Ga melt after the annealing in the Ga melt at 600 °C for 24 h annealing; (d) near the opposite surface of wafer after the 24 h Ga melt annealing. Markers represent 50  $\mu\text{m}$ .

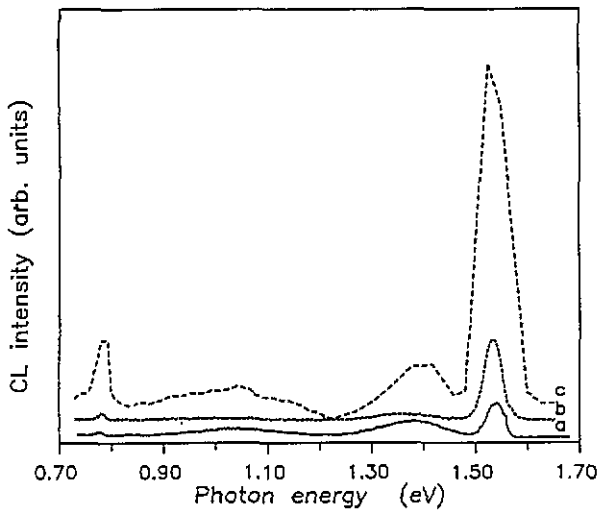
of the wafer volume. Figure 7 shows the typical CL spectra of the 2 h annealed wafers. It is seen that the 1.13 eV and 1.4 eV bands, which dominated the CL spectra of as-grown wafers (figure 6), disappeared over the whole volume of the 2 h annealed wafers with exception of the regions near the surface of the wafers, which was not in contact with the Ga melt. The intensity of the 1.54 eV band decreased by a factor of two to three and four to five respectively in the central part of the wafer cross sections and in the region near the wafer surfaces which were in contact with the Ga melt (figure 7, curves b and a respectively). Simultaneously, the 1.54 eV band intensity increased by three to four times near the opposite surface of the wafers, which was exposed in a vacuum (figure 7, curve c).

Figure 8 shows the typical CL spectra of the 24 h Ga melt annealed wafers. The CL spectra demonstrate the lowest defect density in the central part of the wafer cross sections as after the 2h annealing. In comparison with figure 7, an increase of the 1.4 eV band intensity can be seen in figure 8 over the whole volume of the 24 h annealed wafers. The intensity of the 1.54 eV band increased in the central part of the wafer cross sections and in the region near the wafer surfaces which was in contact with the Ga melt (figure 8, curves b and a respectively) and it decreased near the opposite surface of the wafers (figure 8, curve c).



**Figure 6.** CL spectra recorded at 80 K from a cross section of the as-grown CdTe wafer, with (a) a focused and (b) a defocused electron beam.

The behaviour of the 1.4 eV and 1.54 eV bands, which are presented in figures 7 and 8, can be explained as the result of an in-diffusion of Ga atoms into the wafers from the Ga melt and an out-diffusion of Cd atoms from the wafer surfaces, which were exposed in a vacuum. The Ga in-diffusion provides an increase in the concentration of donors which are Ga atoms



**Figure 7.** CL spectra (80 K, a focused electron beam) recorded from a cross section of the CdTe wafer annealed in the Ga melt at 600°C for 2 h: (a) in the region near the wafer surface which was in contact with the Ga melt; (b) in the central part of cross section; (c) in the region near the wafer surface which was opposite to the Ga melt.

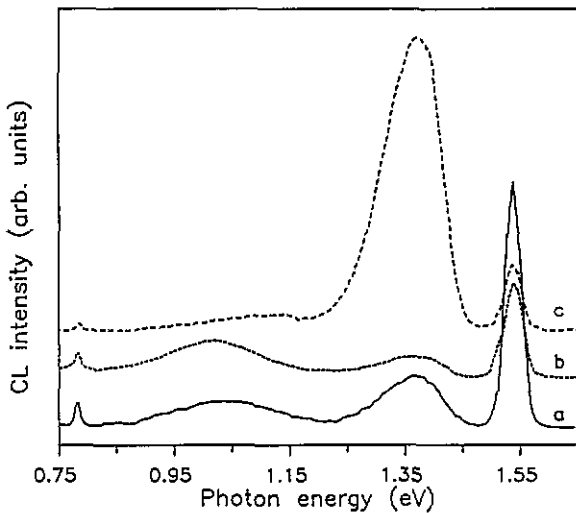


**Figure 8.** CL spectra (80 K, a focused electron beam) recorded from a cross section of the CdTe wafer annealed at 600°C for 24 h: (a) in the region near the wafer surface which was in contact with the Ga melt; (b) in the central part of the cross section; (c) in the region near the wafer surface which was opposite to the Ga melt.

in Cd sites and the group I residual impurities in interstitials [7,8]. Simultaneously, it decreases the concentration of acceptors (Cd vacancies and the group I residual impurities in Cd sites [7,8]) which causes the increase of intensities of the 1.4 eV and 1.54 eV bands near the wafer surfaces in contact with the Ga melt (figure 8, curve a). Near the opposite surface of the wafers, an out-diffusion of Cd atoms is followed by an increase in the concentration of Cd vacancies and a decrease in concentration of the group I residual impurities in interstitials. Due to this, the concentration of acceptors increases and the concentration of donors decreases. That provides an increase of the 1.4 eV band intensity and a decrease of the 1.54 eV band intensity (figure 8, curve c).

Thus, the CL data complement the RS data and justify the necessity of taking into account the doping and out-diffusion processes which occur simultaneously with the elimination of Te precipitates.

### 3.3. Annealing in Cd vapour and in a vacuum

After the annealing of as-grown wafers in Cd vapour for 2 h, the RS and CL spectra and the CL images were found to be similar to those which were seen after the 2 h annealing in the Ga melt (figures 2 and 7 curves b and figure 5(b)). The 24 h annealing in Cd vapour causes a disappearance of Te precipitates in the central part of the wafer cross sections. In this case, the CL images showed a narrow precipitate-free region 100–300  $\mu\text{m}$  thick the boundaries of which were not well defined, unlike after the 24 h annealing in the Ga melt. The reason for such a difference between the Ga melt and Cd vapour annealing procedures could be related to the capability of the Ga melt to dissolve the Te precipitates which migrate to the surface of the wafers during the annealing. After the 24 h annealing in Cd vapour, the CL spectra over the whole volume of the wafers were similar to the one shown in figure 8, curve b. Near both surfaces of the wafers a small increase in the intensities of the 1.4 eV and 1.54 eV bands was seen, which could be due to the dissolution of Te precipitates and the increase in the concentration of the group I residual impurities in interstitials.

After the annealing of the wafers in a vacuum for 2 h or 24 h, the initial RS spectra and CL images (figures 1 and 5(a)) did not change significantly, showing a random distribution of Te precipitates over the whole volume of the wafers. Only an increase in the concentration of Te precipitates was seen near the both surfaces of the wafers, which provided CL images like the one presented in figure 5(d).

These data show an important effect of the ambient (Ga melt, Cd vapour or a vacuum) on the process of elimination of Te precipitates.

## 4. Conclusions

The thermal annealing of the undoped and doped CdTe wafers has been studied in order to eliminate Te precipitates from the wafer volume. Precipitate-free wafers have been obtained by the annealing in the Ga melt in a real time-scale (24 h at 600°C). The annealing was shown to modify drastically the RS and CL spectra and the CL images over the whole volume of the wafers. The kinetics of elimination of Te precipitates was found to be similar in the undoped and doped wafers.

The comparison of the annealing procedures in the Ga melt, or in Cd vapour or in a vacuum has been made to distinguish the effect of the ambient. It was shown that the rate of the elimination process is the highest for the annealing in the Ga melt. Simultaneously with the elimination of Te precipitates, the Ga melt causes the in-diffusion of Ga atoms into the wafers. This implies that the annealing in the Ga melt could be a superior

procedure (e.g. in comparison with the annealing in a graded temperature field [4]) for the elimination of Te precipitates from CdTe wafers in which the Ga doping is not important (e.g. for infrared optics applications) or, on the contrary, it is desired (e.g. for the fabrication of n-i-p structures for nuclear radiation detector [7]).

The RS and CL data in this paper complement our previous findings on the transformation of the photoluminescence spectra of CdTe wafers after thermal annealing procedures [7, 8, 11]. Essentially, the photoluminescence properties reported in [7, 8, 11] have to be attributed to either the space between Te precipitates or the whole volume of the wafers depending on the type and duration of the annealing procedures.

It is also worth noting that in the literature different terms are used for the specification of Te excess in CdTe crystals. For example, to describe similar infrared microscopic images, some authors use the term 'precipitate' [1, 3, 4, 12–15], while others use the term 'inclusions' [2, 18, 19]. In our opinion, this controversy is due to the attempts to compare the crystals grown in essentially different growth conditions. CdTe crystals grown from the Cd-Te melts with a small deviation from stoichiometric composition (e.g. [7]) contain only Te precipitates of well known circular form (figure 5), the size of which depends on the growth rate and post-growth cooling regime; CdTe crystals grown from non-stoichiometric Cd-Te melts contain some additional inclusions which appear because of melt capture at the crystallization front, and their composition and form depend strongly on the melt composition as well as the growth conditions [2, 18, 19]. In this work we have used the term 'precipitate' as the most relevant and we believe that the reported kinetics of elimination of Te precipitates will not be substantially different, in CdTe wafers prepared from crystals grown in non-stoichiometric conditions.

### Acknowledgment

Two of us (NVS and UP) thank research fellowships from the Spanish Ministerio de Educacion y Ciencia.

This work has been supported by DGICYT (project PB93-1256).

### References

- [1] Sen S, Konkel W H, Tighe S J, Bland L G, Sharma S R and Taylor R E 1988 *J. Cryst. Growth* **86** 111–17
- [2] Brion H G, Mewes C, Hahn I and Schaufele U 1993 *J. Cryst. Growth* **134** 281–6
- [3] Jayathirtha H N, Henderson D O, Burger A and Volz M P 1993 *Appl. Phys. Lett.* **62** 573–5
- [4] Vydyanath H R, Ellsworth J A, Parkinson J B, Kennedy J J, Dean B, Johnson C J, Neugebauer G T, Sepich J and Liao P K 1993 *J. Electron. Mater.* **22** 1073–80
- [5] Peters K, Wenzel A and Rudolph P 1990 *Cryst. Res. Technol.* **25** 1107–16 and references therein
- [6] Jones E D, Malzbender J, Mullin J B and Shaw N 1994 *J. Phys.: Condens. Matter* **6** 7499–504
- [7] Sochinskii N V, Serrano M D, Babentsov V N, Tarbaev N I, Garrido J and Diéguez E 1994 *Semicond. Sci. Technol.* **9** 1713–18
- [8] Sochinskii N V, Babentsov V N, Tarbaev N I, Serrano M D and Diéguez E 1993 *Mater. Res. Bull.* **28** 1061–6
- [9] Koralewskii M, Sochinskii N V, Serrano M D, Diéguez E, Garrido J, Lifante G, Noheda B and Gonzalo J A 1994 *Appl. Phys. Commun.* **13** 69–78
- [10] Sochinskii N V, Babentsov V N, Kletskii S V, Serrano M D and Diéguez E 1993 *Phys. Status Solidi a* **140** 445–51
- [11] Sochinskii N V, Serrano M D, Bernardi S and Diéguez E 1994 *Proc. 'Advanced Infrared Technology and Application' (Capri, September 1993)* (Florence: Atti Fond. G.R.) 43–55
- [12] Shin S H, Bajaj J, Moudy L A and Cheung D T 1983 *Appl. Phys. Lett.* **43** 68–70
- [13] Kim W J, Park M J, Kim S U, Lee T S, Kim J M, Song W J and Suh S H 1990 *J. Cryst. Growth* **104** 677–82
- [14] Sochinskii N V, Serrano M D, Diéguez E, Agulló-Rueda F, Pal U, Piqueras J and Fernández P 1995 *J. Appl. Phys.* **77** at press
- [15] Amirtharaj R M and Pollak F H 1984 *Appl. Phys. Lett.* **45** 789–91
- [16] Domínguez-Adome F, Piqueras J and Fernández P 1991 *Appl. Phys. Lett.* **58** 257–9
- [17] Pal U, Piqueras J, Fernández P, Serrano M D and Diéguez E 1994 *J. Appl. Phys.* **76** 3720–3
- [18] Rudolph P, Neubert M and Mühlberg M 1993 *J. Cryst. Growth* **128** 582–7
- [19] Schwarz R and Benz K W 1994 *J. Cryst. Growth* **144** 150–6